Dissociative frustrated multiple ionization of hydrogen chloride in intense femtosecond laser fields

Junyang Ma,[1] Hui Li,[1,*] Kang Lin,[1] Qinying Ji,[1] Wenbin Zhang,[1] Hanxiao Li,[1] Fenghao Sun,[1] Junjie Qiang,[1] Peifen Lu,[1] Xiaochun Gong,[1] and Jian Wu[1,2]

[1]*State Key Laboratory of Precision Spectroscopy, East China Normal University, Shanghai 200062, China*

[2]*Collaborative Innovation Center of Extreme Optics, Shanxi University, Taiyuan, Shanxi 030006, China*

(Received 17 October 2018; published 13 February 2019)

The dissociative frustrated multiple ionization of hydrogen chloride (HCl) molecules in intense femtosecond laser fields is investigated by employing the coincidence measurement technique in cold target recoil ion momentum spectroscopy. Various dissociative frustrated multiple ionization channels caused by populating one or two electrons to highly excited Rydberg states can be clearly distinguished for HCl in linearly polarized intense laser fields. The excited charged fragmentations, depending on their occupied principle quantum numbers, can be either directly identified forming a "knee" structure in the kinetic energy release spectrum, or singly ionized by the weak electric field in the spectrometer, or by blackbody radiation after the conclusion of the laser pulse. The inherent feature of the potential energy curves of HCl plays an important role in the strong-field dissociative frustrated multiple ionization process.

DOI: 10.1103/PhysRevA.99.023414

I. INTRODUCTION

Tunneling ionization is one of the most fundamental manifestations of the interaction between strong laser fields and atomic molecular systems such that the bound electron can escape from the atomic and molecular potentials which are dramatically distorted by the intense oscillating electric fields. It built the foundation for a wide range of fascinating phenomena in strong-field physics such as the high-harmonic generation [1–7], nonsequential double ionization [8–12], and electron diffraction [13–15]. In addition to the tunneling ionization channel, there exists a neutral exit channel when atoms or molecules are exposed to intense laser fields, i.e., the frustrated tunneling ionization (FTI) channel, where the ejected electron cannot obtain enough drift energy from the laser field to overcome the attractive Coulomb potential of the parental nucleus and thus will eventually populate high-lying Rydberg states [16–18]. The underlying physics related to FTI has been explored not only for homonuclear diatomic molecules such as hydrogen [19–23] and nitrogen [24] but also for complex molecular and cluster targets [25–27]. There is a certain probability that the excited neutral or charged fragments formed by recapturing of tunneled electrons can be directly detected by the reaction microscope [20–27]. Moreover, the phenomenon of two Rydberg electrons localizing at two nuclear cores has been observed in argon dimer [28]. Although the dissociative FTI has been observed for various targets, there are still a lot of dissociative excited fragments with very high principal quantum numbers that cannot be detected in a straightforward way. These fragments can be ionized by the weak dc field in the spectrometer or by blackbody radiation (BBR) before they reach the detector and therefore contribute to the signals of different final charged states [29–32]. As a result of this, experimental studies rarely appear for the molecular dissociative frustrated multiple ionization (DFMI) where the underlying physics is yet unclear.

Hydrogen chloride and its isotopes have been investigated as interesting systems with fascinating properties such as large dipole moments in strong laser fields [33–35]. In this work, we study the dissociative multiple ionization channels in HCl by detecting the fragmentations in a reaction microscope when the molecules interact with intense femtosecond near-infrared laser pulses. Since the hydrogen can only be ionized to form the singly ionized charge state, the multiple ionization of HCl provides us an ideal covalent bond molecule to investigate the multiple population of the electrons on the ejected chloride fragment. The coincidence measurement allows us to unambiguously identify the DFMI signals through analyzing the kinetic energy release (KER) and momentum angular distributions for different final charge states.

II. EXPERIMENTAL SETUPS

The momentum distributions of the fragmenting electrons and ions from HCl exposed to the intense femtosecond laser pulses were measured in coincidence in a cold target recoil ion momentum spectroscopy (COLTRIMS) [36,37] as schematically illustrated in Fig. 1. A beam of femtosecond pulses (25 fs, 790 nm, 10 kHz) produced from a multipass Ti:sapphire amplifier was focused onto a HCl molecular beam (propagates along the y direction) by a concave reflection mirror ($f = 75$ mm) inside the vacuum chamber. The supersonic gas jet was produced by coexpanding a mixture of 5% HCl and 95% He through a 30-μm nozzle with a driving pressure of about 2.0 bars. The laser field polarization was adjusted using a quarter-wave plate (QWP) and a half-wave plate (HWQ). The peak intensities of the linearly and circularly polarized laser fields in the interaction region were estimated to be $\sim 5\times10^{14}$ and $\sim 9\times10^{14}$ W/cm^2, respectively. According

*hli@lps.ecnu.edu.cn

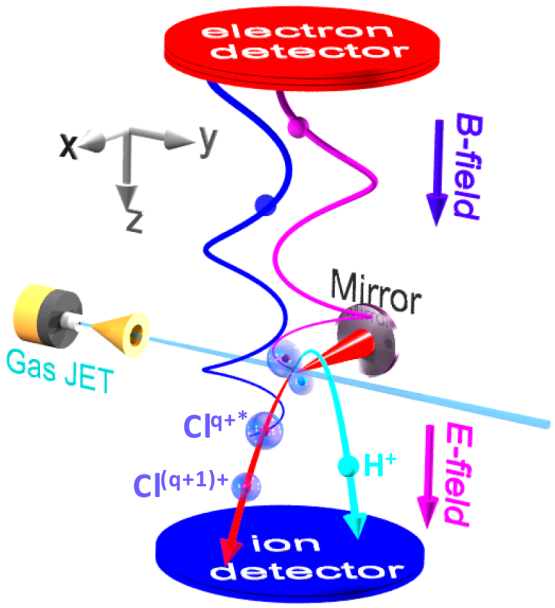

FIG. 1. Schematic diagram of the experimental setup.

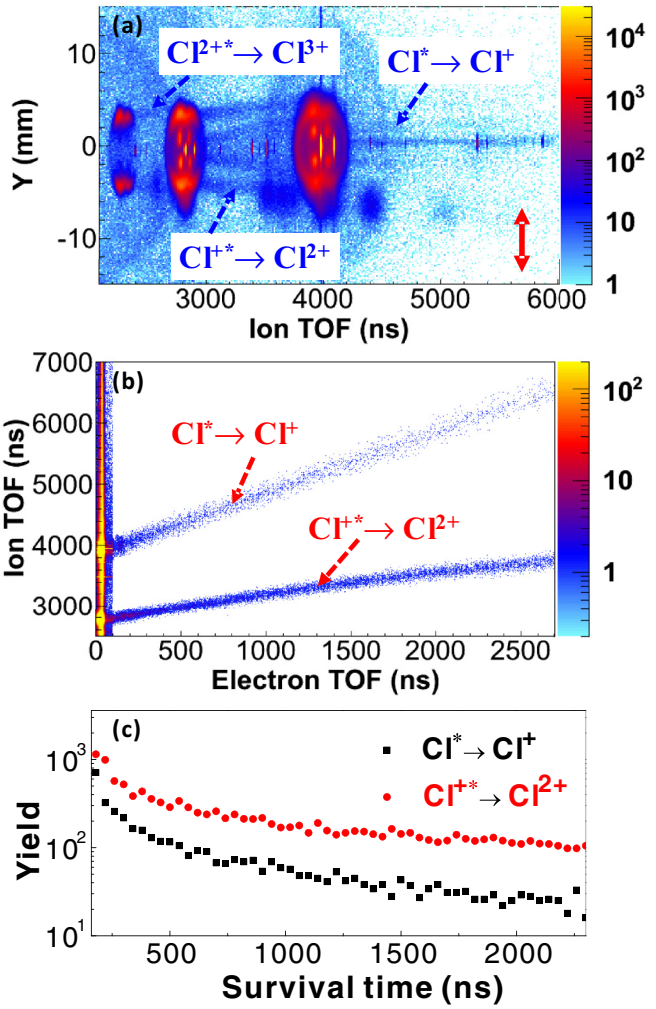

FIG. 2. (a) Ionic yields as a function of times of flight and displacements in the y direction from HCl interacting with linearly polarized femtosecond laser field. The polarization direction is indicated by the red arrow. A couple of postpulse ionization channels for the highly excited ion fragments are pointed out by the blue dashed arrows. (b) The PEPICO spectrum of the HCl$(1, q^* \rightarrow q+1)$ channels $(q = 0, 1)$. (c) Retrieved survival time distributions of the chloride ions from the HCl$(1, q^* \rightarrow q+1)$ channels $(q = 0, 1)$.

to the first ionization potential of HCl (about 12.7 eV), the corresponding Keldysh parameters for the linear and circular polarization conditions were estimated to be ∼0.48 and ∼0.35, both lying in the tunneling regime. In the spectrometer, the emitted ions were accelerated by the static dc field (∼22.2 V/cm), and a homogeneous magnetic field of 13.0 G was applied to guide the electrons. On the other hand, the produced excited neutral fragments in the dissociative frustrated ionization of HCl can also be detected if they fly toward the ion detector and exhibit initial energies larger than the work function of the microchannel plate (MCP) [20]. Other neutral fragmentations with lower energy or larger incidence angle on the MCP cannot be effectively detected. Three-dimensional (3D) momentum distributions of the fragmentations can be reconstructed from the times of flight (TOFs) and the positions of the impacts in the postanalysis procedures.

III. RESULTS AND DISCUSSIONS

Figure 2(a) shows the measured ion yield from HCl as a function of TOF and y position when the laser field is linearly polarized along the y axis. Besides the major signal distributions around the TOFs of 2253, 2752, and 3891 ns, corresponding to dissociative fragments of Cl^{3+}, Cl^{2+}, and Cl^+ from HCl, there exist special distributions extending from the main distributions of, e.g., the $Cl^{(q+1)+}$ fragment, all the way toward the lower charged state of Cl^{q+}, as pointed out by the blue dashed arrows in Fig. 2(a). In this plot, we obtain two pairs of such distributions between the Cl^+ and the Cl^{2+} peaks (located between 2752 and 3891 ns), of which the outer line extends within the displacement of about ±2.8 mm to ±5.5 mm in the y direction (indicated by the "$Cl^{+*} \rightarrow Cl^{2+}$" in the figure) while the inner pair lies at smaller y positions with $|y| < 2.8$ mm. Another pair of the extension can be distinguished between the signals at about 2253 ns (Cl^{3+}) and 2752 ns (Cl^{2+}) which is indicated by the "$Cl^{2+*} \rightarrow Cl^{3+}$". Moreover, there is a long linear distribution starting from the Cl^+ peak (around 3891 ns) and occupying the long TOF region along the $y = 0$ axis (indicated by the "$Cl^* \rightarrow Cl^+$"). Within all these elongated distributions, the inner line pair (with smaller displacements in the y direction) between the TOF of the Cl^+ and the HCl^{2+} (which is close to the TOF of Cl^{2+}) can be attributed to the delayed Coulomb explosion of the long-lived HCl^{2+} ions during the flight to the detector [38]. The outer line and other extended distributions are, however, formed through a different mechanism which will be focused on through this paper.

In the strong-field dissociative ionization of HCl molecules by using linearly polarized femtosecond pulses, there is a certain probability that the released electrons driven by the external electric field be finally recaptured by the extending Rydberg orbitals of the dissociating compounds. These recaptured electrons can occupy highly excited Rydberg states

localizing very close to the ionization threshold. If the electrons populate the states with high principle quantum numbers, they have a certain chance to be ionized by the dc field in the spectrometer or by the BBR before they reach the detector [29,31]. To provide a rough estimation, the lowest principle quantum number of a neutral Rydberg state (n_F) being ionized can be calculated using the saddle-point approximation of the field ionization threshold which is expressed as $F_{\rm dc} = 1/(9n_F^4)$ in atomic units [29,39], where $F_{\rm dc}$ is the field strength. For $F_{\rm dc} = 22.2\,{\rm V/cm}$, Rydberg electrons with $n > n_F = 70$ can be freed through over-the-barrier or tunneling ionization for neutral Rydberg atoms. For the case of charged Rydberg states, the influence on the charge needs to be considered as $F_{\rm dc} = Z^3/(9n_F^4)$ where Z represents the charge state [40]. On the other hand, the influence from the photoionization by BBR mainly dominates the very long emission times and the induced ionization rate would be orders of magnitude lower than that induced by the dc field in single ionization [29,31]. In the measurements of multiple ionization the influence from BBR radiation is very limited, and thus will be neglected in the following discussions.

Starting from two extreme cases, one possibility is that the dissociative excited fragments Cl^{q+*} are formed by electron recapture to the chloride core ionized by the dc field immediately after the interaction with femtosecond laser pulses; then the outcoming ion TOF will be the same as that of the $Cl^{(q+1)+}$. On the other hand, there is the possibility that the excited fragments Cl^{q+*} are ionized right before they arrive at the ion detector; thus the detected TOF will be the same as that of Cl^{q+}. The fragments which are dc field ionized in between these two extreme cases will occupy the linear distributions between the TOF peaks of Cl^{q+} and $Cl^{(q+1)+}$ as shown in Fig. 2(a). In particular, for the case of $q = 0$, the dc-field-ionized fragments Cl^+ ($Cl^* \rightarrow Cl^+ + e^-$) will take a longer flight time toward the detector compared to the Cl^+ fragments generated in laser-molecule interactions since dc field acceleration is absent for neutral particles, which can explain the linear extension of the $Cl^* \rightarrow Cl^+$ process. All the above-mentioned processes involving electron-recapture-induced excitation and postpulse field ionization can be formulated as $HCl \rightarrow H^+ + Cl^{q+*} + (q+1)e^- \rightarrow H^+ + Cl^{(q+1)+} + (q+2)e^-$, and will be denoted as HCl $(1, q^* \rightarrow q+1)$ channels. In our experimental technique, 4π sr acceptance angle can be achieved for the detection of higher-order excited fragmentations, while the acceptance angle of neutral excited particles is limited to a small range (0.9π sr) [20]. In this sense, reaction microscopy provides a power tool to explore the DFMI process in complex molecules.

One of the questions related to the DFMI is when would the dissociative highly excited fragments Cl^{q+*} be ionized during their flight toward the detector. This can be retrieved from measuring the photoelectron photoion coincidence (PEPICO) spectra. As displaced in Fig. 2(b), the long-lived highly excited fragments Cl^{q+*} can be easily distinguished with diagonal distributions. Due to the extremely low signal rate of the higher charged channels, only the HCl $(1, 0^* \rightarrow 1)$ and HCl $(1, 1^* \rightarrow 2)$ channels will be discussed here. The survival time of the fragments Cl^{q+*} can be estimated as $T_{\rm elec}$–T_0, where T_0 is the most probable TOF for electrons released in the strong-field ionization (here $T_0 = 36\,{\rm ns}$); $T_{\rm elec}$ is the measured TOF of individual electrons. The retrieved survival times of the fragments Cl^{q+*} in the HCl$(1, q^* \rightarrow q+1)$ channels ($q = 0, 1$) are plotted in Fig. 2(c). Compared to the early measurements [29], the delayed ionization shown in Fig. 2(c) is dominated by a single exponential decay that could stem from dc-field-induced over-the-barrier or tunneling ionization. Decay rates of 5.0×10^{-3} and $6.9\times10^{-3}\,{\rm ns}^{-1}$ can be obtained for the HCl $(1, 0^* \rightarrow 1)$ and the HCl $(1, 1^* \rightarrow 2)$ channels by fitting the data with an exponential formulism. In our study, we did not observe significant contribution from the BBR ionization which, in principle, occupies the signal at much longer flying times.

On the other hand, one may ask about the influence on the KER and momentum angular distributions by electron recapture and the postpulse ionization processes in the DFMI scenario. Figures 3(a) and 3(b) show the measured ion yields for the HCl$(1, q^* \rightarrow q+1)$ channels ($q = 0, 1$) as a function of the ion TOF and y positions which are selected based on momentum conservation of the measured nuclear fragments. The tiny recoil momentum of the ejected Rydberg electrons from the dc-field-induced ionization of the Cl^{q+*} fragments is neglected here. The retrieved KER and momentum angular distributions are shown in Figs. 3(c)–3(f) (the red solid curves). For comparison, the corresponding results from the Coulomb exploded HCl $(1, 1)$ and HCl $(1, 2)$ channels [i.e., the $HCl \rightarrow H^+ + Cl^{q+} + (q+1)e^-$ channels, denoted as HCl $(1, q)$] measured under the same experimental condition are shown by the black solid curves. We can see that similar KER spectra and angular distributions were obtained for the HCl$(1, q^* \rightarrow q+1)$ and HCl$(1, q+1)$ channels. The KER distributions of the dissociative double ionization channel, i.e., the HCl $(1, 1)$ channel, show nice agreement with previous measurements driven by femtosecond laser fields [35,38]. However, the fine structure cannot be well distinguished for the DFMI channels, which might be attributed to the limited statistics of the acquired data. We can see in Fig. 3(e) that the two channels exhibit similar narrow angular distributions along the laser polarization direction (along 90° and 270°) which indicate that the dissociation process took place within a short timescale. This provides further evidence for the suggested mechanism such that the electron is populated to an excited Rydberg state when dissociation is approaching its end; thus the modification on the ion KER and its momentum angular distributions will not be significant. The situation is similar for the HCl $(1, 1^* \rightarrow 2)$ and HCl $(1, 2)$ channels, as shown in Figs. 3(d) and 3(f). In brief, the formation of the HCl$(1, q^* \rightarrow q+1)$ DFMI channels (as shown in Fig. 1) can be described as follows: The HCl molecule undergoes multiple ionization and dissociates into a H^+ and a $Cl^{(q+1)+}$ ion when exposed to a linearly polarized strong laser field. By populating an electron to the chloride side, a highly excited fragment ion Cl^{q+*} can be formed. In the case that Rydberg states with high principle quantum numbers are occupied, the excited fragment Cl^{q+*} can be further ionized under the influence of a weak spectrometer field and will emit a Rydberg electron that will thus be detected as $Cl^{(q+1)+}$. The similar angular distribution characters between the HCl$(1, q^* \rightarrow q+1)$ and HCl$(1, q+1)$ channels show that the dissociative fragments H^+ and Cl^{q+*} are produced on

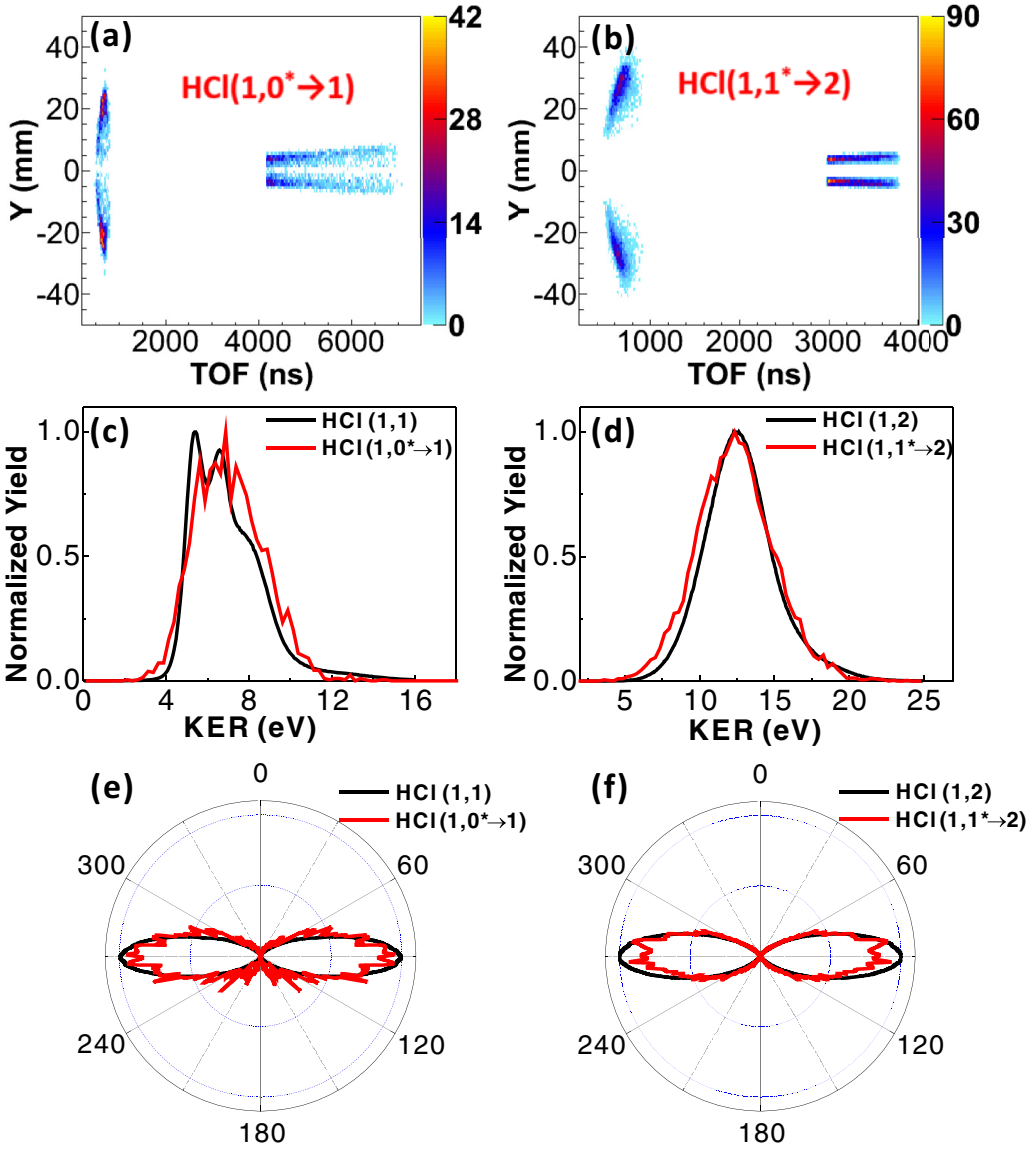

FIG. 3. (a,b) Ionic yields as a function of TOF and y positions for the HCl$(1, q^* \rightarrow q+1)$ channels ($q = 0, 1$). (c,d) The KER spectra of the HCl$(1, q+1)$ and the HCl$(1, q^* \rightarrow q+1)$ channels in linearly polarized laser field. ($q = 0, 1$). (e,f) Polar plots of the momentum angular distributions for the HCl$(1, q+1)$ and the HCl$(1, q^* \rightarrow q+1)$ channels ($q = 0, 1$) in the polarization plane (the y−z plane).

a femtosecond timescale, which is a different scenario compared to the delayed dissociative double ionization channel of HCl [38].

Up to now we have discussed the DFMI channels related to highly excited Rydberg states with large principle quantum numbers. Then one may ask, what will happen to the dissociative excited chloride fragments Cl^{q+*} with low principal quantum numbers? These fragments surviving in the post-pulse ionization will be detected in the HCl $(1, q)$ channels. Figures 4(a) and 4(b) show the measured KER spectra of the HCl $(1, q)$ Coulomb explosion channels in both the linearly and circularly polarized laser fields. In Fig. 4(a), we can see clear "knee" structures showing at the high-energy side of the main peak for the HCl $(1, q)$ channels. Interestingly, the knee structure from the HCl $(1, q)$ channels approximately lines up with the main peak of the HCl$(1, q+1)$ channels, which is manifested by the green guiding dashed lines in the plot. This indicates that the signal in the knee structure may be from the surviving highly excited DFMI channel with lower principle quantum numbers. Sudden localization of the Rydberg electron to the chloride core did not initiate significant modification on the KER distributions which indicates that the Rydberg population may take place approaching the end of the dissociation such that the potential energy curves of involved final charge states do not exhibit much difference [28]. The knee shape is absent in the circularly polarized case as shown in Fig. 4(b) which provides a good verification for the FTI assumption. This technique allows us to distinguish the HCl $(1, q^*)$ signal from that of the pure Coulomb exploded channels HCl $(1, q)$.

Finally, the cases where Rydberg electron localizing on the hydrogen core, thus forming the DFMI channels

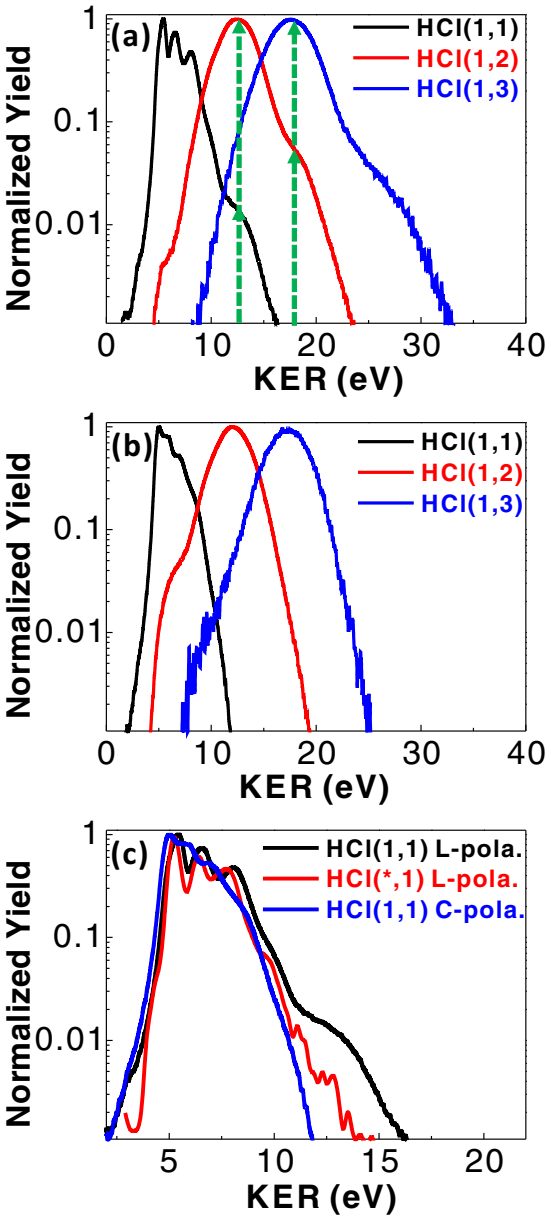

FIG. 4. (a) The KER spectra for the HCl $(1,\ q)$ $(q = 1, 2, 3)$ channels in linearly polarized laser field. (b) The same as (a) but for circular polarization. (c) The KER spectra for the HCl $(^*, 1)$ channel in linearly polarized laser field (along z axis) and for the HCl $(1, 1)$ channel in both linearly and circularly polarized cases.

$[\mathrm{HCl} \rightarrow \mathrm{H}^* + \mathrm{Cl}^{q+} + qe^-$, labeled as the HCl $(^*, q)$ channel], will be briefly introduced. In our measurements we obtain the signals for the HCl $(^*, 1)$ channel, of which the KER spectrum is presented in Fig. 4(c). The KER distributions from the HCl $(1, 1)$ channel are plotted in the same figure for both linear and circular polarizations. By comparing with the data from circular polarization, the knee structure can be well recognized for both the HCl $(1, 1)$ and the HCl $(^*, 1)$ channels. According to the above discussions on Fig. 4(a), the KER distribution in the knee region of the HCl $(1, 1)$ channel can be attributed to electron recapture to the hydrogen core. Interestingly, the knee structure around 11–14 eV obtained for the HCl $(^*, 1)$ channel could be from recapture of two Rydberg electrons by both the chloride and the hydrogen cores. In principle, the probability for such dual-recapture hypothesis will be much smaller than that for the single-recapture case, which qualitatively agree with the smaller knee observed for the HCl $(^*, 1)$ channel compared to that from the HCl $(1, 1)$ channel. The postpulse ionization of the exited H^* fragmentations by the dc electric field or by BBR is not observed in the present experiment which might be due to the fact that the principle quantum numbers occupied by the H^* fragments are too low. In general, our measurement shows higher probability for the localization of the Rydberg electron at the nuclear fragment with the higher charge state, which agrees with early experimental studies on the multiple electron recapture of the Ar dimer [28].

IV. CONCLUSION

In summary, we have investigated the DFMI of HCl in intense femtosecond laser fields. By analyzing the KER and momentum angular distributions for several final charge states obtained in coincidence measurements, significant DFMI signals can be distinguished for linear polarization. The general scenario of DFMI is found to be that the HCl molecules undergo dissociative multiple ionization in the strong-field regime while some of the tunneled electrons can be populated to high-lying Rydberg states of the dissociating fragments. In our measurement, electron recapture by both the chloride side and the hydrogen side can be obtained. The excited charged ions can be detected directly (when occupying states with low principle quantum numbers) or will be ionized during their flight toward the detector (when the states with high principle quantum numbers are occupied) and are thus measured in different final charge states. In the former case, a "knee" structure can be formed in the KER spectra of which the energy coincides with the KER distributions of higher charged states. We find that the final KER distributions can be rarely influenced by the electron recapture or by the postpulse ionization processes. This might stem from the inherent feature of the HCl molecule such that potential energy curves of the involving charge states exhibit very small differences; thus the sudden jumping between them caused by electron recapture does not induce significant modification on the KER. Our method based on coincidence measurement provides a powerful tool to reveal the underlying physics of DFMI processes in complex molecular systems.

ACKNOWLEDGMENTS

This work is supported by the National Key R&D Program of China (Grant No. 2018YFA0306303), the National Natural Science Fund of China (Grants No. 11704124, No. 11425416, No. 61690224, No. 11761141004, and No. 11834004), the Shanghai Sailing Program (Grant No. 17YF1404000), and the 111 Project of China (Grant No. B12024). J.M. acknowledges the financial support from the China Scholarship Council (CSC).

[1] P. B. Corkum, Phys. Rev. Lett. **71**, 1994 (1993).

[2] M. Drescher, M. Hentschel, R. Kienberger, G. Tempea, C. Spielmann, G. Reider, P. Corkum, and F. Krausz, Science **291**, 1923 (2001).

[3] A. Fleischer, O. Kfir, T. Diskin, P. Sidorenko, and O. Cohen, Nat. Photon. **8**, 543 (2014).

[4] O. Kfir, P. Grychtol, E. Turgut, R. Knut, D. Zusin, D. Popmintchev, T. Popmintchev, H. Nembach, J. M. Shaw, A. Fleischer, H. Kapteyn, M. Murnane, and O. Cohen, Nat. Photon. **9**, 99 (2015).

[5] K. J. Schafer, B. Yang, L. F. DiMauro, and K. C. Kulander, Phys. Rev. Lett. **70**, 1599 (1993).

[6] L. He, P. Lan, A.-T. Le, B. N. Wang, B. C. Wang, X. Zhu, P. Lu, and C. D. Lin, Phys. Rev. Lett. **121**, 163201 (2018).

[7] M. Huppert, I. Jordan, D. Baykusheva, A. von Conta, and H. J. Wörner, Phys. Rev. Lett. **117**, 093001 (2016).

[8] D. N. Fittinghoff, P. R. Bolton, B. Chang, and K. C. Kulander, Phys. Rev. Lett. **69**, 2642 (1992).

[9] B. Walker, B. Sheehy, L. F. DiMauro, P. Agostini, K. J. Schafer, and K. C. Kulander, Phys. Rev. Lett. **73**, 1227 (1994).

[10] N. Camus, B. Fischer, M. Kremer, V. Sharma, A. Rudenko, B. Bergues, M. Kubel, N. G. Johnson, M. F. Kling, T. Pfeifer, J. Ullrich, and R. Moshammer, Phys. Rev. Lett. **108**, 073003 (2012).

[11] X. Gong, Q. Song, Q. Ji, H. Pan, J. Ding, J. Wu, and H. Zeng, Phys. Rev. Lett. **112**, 243001 (2014).

[12] B. Bergues, M. Kubel, N. G. Johnson, B. Fischer, N. Camus, K. J. Betsch, O. Herrwerth, A. Senftleben, A. M. Sayler, T. Rathje, T. Pfeifer, I. Ben-Itzhak, R. R. Jones, G. G. Paulus, F. Krausz, R. Moshammer, J. Ullrich, and M. F. Kling, Nat. Commun. **3**, 813 (2012).

[13] M. Meckel, D. Comtois, D. Zeidler, A. Staudte, D. Pavicic, H. C. Bandulet, H. Pepin, J. C. Kieffer, R. Dorner, D. M. Villeneuve, and P. B. Corkum, Science **320**, 1478 (2008).

[14] C. I. Blaga, J. Xu, A. D. DiChiara, E. Sistrunk, K. Zhang, P. Agostini, T. A. Miller, L. F. DiMauro, and C. D. Lin, Nature (London, UK) **483**, 194 (2012).

[15] M. G. Pullen, B. Wolter, A.-T. Le, M. Baudisch, M. Hemmer, A. Senftleben, C. D. Schröter, J. Ullrich, R. Moshammer, C. D. Lin, and J. Biegert, Nat. Commun. **6**, 7262 (2015).

[16] T. Nubbemeyer, K. Gorling, A. Saenz, U. Eichmann, and W. Sandner, Phys. Rev. Lett. **101**, 233001 (2008).

[17] H. Zimmermann, S. Meise, A. Khujakulov, A. Magaña, A. Saenz, and U. Eichmann, Phys. Rev. Lett. **120**, 123202 (2018).

[18] A. von Veltheim, B. Manschwetus, W. Quan, B. Borchers, G. Steinmeyer, H. Rottke, and W. Sandner, Phys. Rev. Lett. **110**, 023001 (2013).

[19] H. Price, C. Lazarou, and A. Emmanouilidou, Phys. Rev. A **90**, 053419 (2014).

[20] W. Zhang, Z. Yu, X. Gong, J. Wang, P. Lu, H. Li, Q. Song, Q. Ji, K. Lin, J. Ma, H. X. Li, F. Sun, J. Qiang, H. Zeng, F. He, and J. Wu, Phys. Rev. Lett. **119**, 253202 (2017).

[21] J. McKenna, S. Zeng, J. J. Hua, A. M. Sayler, M. Zohrabi, N. G. Johnson, B. Gaire, K. D. Carnes, B. D. Esry, and I. Ben-Itzhak, Phys. Rev. A **84**, 043425 (2011).

[22] B. Manschwetus, T. Nubbemeyer, K. Gorling, G. Steinmeyer, U. Eichmann, H. Rottke, and W. Sandner, Phys. Rev. Lett. **102**, 113002 (2009).

[23] W. Zhang, H. Li, X. Gong, P. Lu, Q. Song, Q. Ji, K. Lin, J. Ma, H. X. Li, F. Sun, J. Qiang, H. Zeng, and J. Wu, Phys. Rev. A **98**, 013419 (2018).

[24] T. Nubbemeyer, U. Eichmann, and W. Sandner, J. Phys. B **42**, 134010 (2009).

[25] A. Chen, M. F. Kling, and A. Emmanouilidou, Phys. Rev. A **96**, 033404 (2017).

[26] B. Manschwetus, H. Rottke, G. Steinmeyer, L. Foucar, A. Czasch, H. Schmidt-Böcking, and W. Sandner, Phys. Rev. A **82**, 013413 (2010).

[27] X. Xie, C. Wu, H. Liu, M. Li, Y. Deng, Y. Liu, Q. Gong, and C. Wu, Phys. Rev. A **88**, 065401 (2013).

[28] J. Wu, A. Vredenborg, B. Ulrich, L. Ph. H. Schmidt, M. Meckel, S. Voss, H. Sann, H. Kim, T. Jahnke, and R. Dörner, Phys. Rev. Lett. **107**, 043003 (2011).

[29] S. Larimian, S. Erattupuzha, C. Lemell, S. Yoshida, S. Nagele, R. Maurer, A. Baltuška, J. Burgdörfer, M. Kitzler, and X. Xie, Phys. Rev. A **94**, 033401 (2016).

[30] T. F. Gallagher and W. E. Cooke, Phys. Rev. Lett. **42**, 835 (1979).

[31] S. Larimian, C. Lemell, V. Stummer, J. W. Geng, S. Roither, D. Kartashov, L. Zhang, M. X. Wang, Q. Gong, L. Y. Peng, S. Yoshida, J. Burgdörfer, A. Baltuška, M. Kitzler, and X. Xie, Phys. Rev. A **96**, 021403(R) (2017).

[32] E. Diesen, U. Saalmann, M. Richter, M. Kunitski, R. Dörner, and J. M. Rost, Phys. Rev. Lett. **116**, 143006 (2016).

[33] H. Akagi, T. Otobe, A. Staudte, A. Shiner, F. Turner, R. Dörner, D. M. Villeneuve, and P. B. Corkum, Science **325**, 1364 (2009).

[34] I. Znakovskaya, P. von den Hoff, N. Schirmel, G. Urbasch, S. Zherebtsov, B. Bergues, R. de Vivie-Riedle, K.-M. Weitzel, and M. F. Kling, Phys. Chem. Chem. Phys. **13**, 8653 (2011).

[35] H. Li, X. M. Tong, N. Schirmel, G. Urbasch, K. J. Betsch, S. Zherebtsov, F. Süßmann, A. Kessel, S. A. Trushin, G. G. Paulus, K.-M. Weitzel, and M. F. Kling, J. Phys. B **49**, 015601 (2016).

[36] J. Ulrich, R. Moshammer, A. Dorn, R. Dörner, L. Ph. H. Schmidt, and H. Schmidt-Böcking, Rep. Prog. Phys. **66**, 1463 (2003).

[37] R. Dörner, V. Mergel, O. Jagutzki, L. Spielberger, J. Ullrich, R. Moshammer, and H. Schmidt-Böcking, Phys. Rep. **330**, 95 (2000).

[38] J. Ma, H. Li, K. Lin, Q. Song, Q. Ji, W. Zhang, H. X. Li, F. Sun, J. Qiang, P. Lu, X. Gong, H. Zeng, and J. Wu, Phys. Rev. A **97**, 063407 (2018).

[39] H. Lv, W. Zuo, L. Zhao, H. Xu, M. Jin, D. Ding, S. Hu, and J. Chen, Phys. Rev. A **93**, 033415 (2016).

[40] F. A. Ilkov, J. E. Decker, and S. L. Chin, J. Phys. B **25**, 4005 (1992).